PROGRESS IN COLOR, COLORANTS AND COATINGS

available online @ www.pccc.icrc.ac.ir

Progress in Color Colorants Coating 19 (2026), 417-434

Ministry of Science, Research and Technology
Institute for Color Science & Technology

Effect of PDMS Anti-Blocking Agent in Water-Based Coatings on the Performance of Paper Substrates for Sustainable Packaging

M. Muryeti*, S. Nur Halisa
Department of Industrial Printing and Packaging Technology, Politeknik Negeri Jakarta, P.O. Box: 16400, Depok, Indonesia.

ARTICLE INFO

Article history:
Received: 05 Sept 2025
Final Revised: 15 Feb 2026
Accepted: 17 Feb 2026
Available online: 03 May 2026

Keywords:
Anti-blocking agent
Paper substrate
Polydimethylsiloxane (PDMS)
Water-based coating

ABSTRACT

Cellulose-based paper is widely used in sustainable food packaging; however, its inherent limitations in barrier and mechanical properties restrict broader application. This study investigates the role of polydimethylsiloxane (PDMS) as an anti-blocking agent in water-based coatings applied to ivory board, kraft paper, and machine-glazed (MG) paper. Three coating formulations were evaluated: a control without PDMS (STD), and formulations containing 0.2 g of PDMS (T-1) and 0.5 g of PDMS (T-2). Coating performance was assessed for blocking resistance, rheological stability, surface friction, coating integrity, barrier properties, and mechanical performance under different storage conditions. The results demonstrate that PDMS incorporation significantly improves anti-blocking behavior, reduces the coefficient of friction, and enhances mechanical durability without compromising water resistance. The formulation with higher PDMS content (T-2) exhibited the most balanced and stable performance during storage, showing improved surface uniformity, lower friction, and enhanced sealing and rub resistance. Substrate-dependent behavior was observed: smooth, dense papers favored uniform surface film formation, while porous substrates promoted coating penetration and mechanical interlocking. These findings highlight the importance of optimizing PDMS concentration and substrate selection to develop high-performance, eco-friendly paper-based coatings for sustainable packaging applications. Prog Color Colorants Coat. 19 (2026), 417-434© Institute for Color Science and Technology.

1. Introduction

Cellulose-based paper is widely used in food packaging due to its flexibility, biodegradability, and sustainable sourcing from natural cellulose resources [1]. This material presents a more environmentally responsible alternative to traditional packaging options, as highlighted by studies from the Institute of Energy and Environment in Germany, which demonstrate the relatively low ecological impact of paper-based packaging compared to plastics and other conventional materials. Nonetheless, certain inherent limitations, such as inadequate barrier properties [2], low mechanical strength, elevated porosity, and limited microbial resistance, hinder the direct applicability of paper in food packaging, potentially compromising the shelf life of packaged products [3].

To overcome these limitations, surface coating has emerged as an effective and economical strategy to enhance the functional performance of paper substrates. The application of polymer-based coatings can significantly improve barrier properties while preserving the recyclability and biodegradability of paper [4]. In

*Corresponding author: * muryeti@grafika.pnj.ac.id
https://doi.org/10.30509/pccc.2026.167649.1442

parallel with technological development, the global packaging coatings market has shown steady growth, reflecting increasing industrial demand for functional coated paper materials [5]. Nevertheless, beyond barrier performance, practical issues related to processing and storage must also be carefully addressed.

One critical property influencing the handling and usability of coated paper is blocking behavior, defined as the tendency of coated surfaces to adhere to one another under the combined effects of pressure, temperature, and storage time [6]. Excessive blocking can lead to permanent adhesion between paper layers or rolls, causing material waste, reduced processing efficiency, and operational challenges during storage and transportation [7]. Therefore, the incorporation of anti-blocking functionality is essential to ensure smooth unwinding, handling, and long-term performance of coated paper products [8].

Polydimethylsiloxane (PDMS) has been widely utilized in coating formulations due to its low surface energy, chemical inertness, thermal stability, and flexibility. Previous studies have demonstrated that PDMS-based coatings can significantly enhance the water- and oil-barrier properties of paper substrates, providing a promising and environmentally friendly alternative to fluorinated coating systems [9]. In addition, PDMS is commonly employed as a multifunctional additive to reduce surface friction, minimize interlayer adhesion [10], and improve resistance to pressure and mechanical stress during storage and handling [11]. Structurally,PDMS is a silicon-based polymer with a flexible –Si–O– backbone, high thermal stability, excellent chemical resistance[12], biocompatibility [13], ease of use, and good gas permeability [14]. Its inherently low surface tension (≈21–22 mN/m) and strong adhesion to substrates [15] promote the formation of continuous, dense coatings on smooth surfaces [16]. Moreover, PDMS is an inert material and commercially available at a relatively low cost [17]. These advantages have enabled its extensive use in the fabrication of superhydrophobic coatings on the surfaces of various substrates, such as metallic [18], cotton, paper [19], and wood [20].

Although the role of slip and anti-blocking agent has been extensively investigated in polymer-based packaging films, their application in paper-based coating systems remains comparatively limited. Existing studies on coated paper primarily emphasize barrier performance. In contrast, practical performance metrics such as blocking resistance, coefficient of friction, rub resistance, coating uniformity, and surface stability under different storage conditions have received considerably less attention [8, 21]. Moreover, the combined effects of coating formulation, additive concentration, substrate characteristics, and aging behavior in water-based, environmentally friendly systems remain poorly understood. Despite growing interest in functional paper coatings, systematic investigations of PDMS-based anti-blocking agent in water-based systems across different paper substrates under realistic storage conditions remain scarce.

In this study, the effects of PDMS-based anti-blocking agent in water-based coatings were systematically investigated on three paper substrates: ivory board, kraft paper, and MG paper. Key performance parameters, including blocking resistance, viscosity, solid content, coating weight, surface morphology, density, water and oil resistance, coefficient of friction, sealing strength, and rub resistance, were evaluated. Statistical analysis was conducted using ANOVA at a 95 % confidence level ($p < 0.05$). By integrating rheological behavior, substrate-dependent absorption, and functional performance during storage, this work provides new insights into the optimization of eco-friendly coating systems for sustainable paper-based packaging applications.

2. Experimental

2.1. Preparation of water-based coatings

In this research, the anti-blocking agent was incorporated into a standard coating formulation to develop water-based coatings. The formulation without polydimethylsiloxane (PDMS) served as the standard (STD), while those containing 0.2 g and 0.5 g of PDMS were designated as T-1 and T-2, respectively. Before testing, all coatings were thoroughly mixed to achieve homogeneity. The experimental samples, encompassing various substrate types and coating compositions, are detailed in Table 1.

Table 1: Coating formulation codes and PDMS dosages.

Formulation Code	PDMS (g)
STD	0
T-1	0.2
T-2	0.5

2.2. Evaluation of storage stability

Storage stability was evaluated by aging the coatings at 40 °C for 14 and 28 days. The temperature range used in this study (25–40 °C) reflects typical industrial storage conditions. The physical and chemical stability of the coatings was monitored during storage.

2.3. Coating application

Coatings were applied to paper substrates using a bar coater. The formulation was dispensed at one end of the substrate and evenly spread across the surface under constant pressure. The coated papers were then dried in a hot-air dryer under controlled conditions. The resulting dry coating thickness was approximately 5–20 μm, which is typical for bar-coated paper substrates. Coating thickness and uniformity were regulated by adjusting the bar wire diameter and coating speed, ensuring consistent film formation and reproducible performance.

2.4. Blocking resistance test

Blocking resistance was assessed as the tendency of coated substrates to adhere under defined load, temperature, and humidity conditions. Tests were conducted in accordance with TAPPI T477 'Blocking Resistance of Paper and Flexible Materials' and ASTM D918-99 'Standard Test Method for Blocking Resistance of Paper and Paperboard', under conditions of 38-60 °C, 44-75 % relative humidity, and 0.5 psi for 21 ± 1 h, simulating industrial-scale conditions for coated papers. In this study, coated substrates were stacked with the coated surface facing the uncoated side, subjected to a 45 kg load, and incubated at 50 °C and 65 % RH for 5 h in a humidity chamber. After incubation, peel tests were performed to evaluate interlayer adhesion. Blocking resistance was quantified using a five-point scale (Table 2), where 1 represents very poor resistance, and 5 indicates excellent resistance.

2.5. Viscosity

Viscosity measurements were performed using a Zahn Cup No. 3 viscometer over a temperature range of 25 to 40 °C, which represents typical industrial processing conditions. The viscosity was determined from the time required for the liquid to flow through the orifice at the bottom of the cup. All measurements were conducted in triplicate, and the results are reported as mean values.

2.6. Solid content

The coating's solid content was determined by gravimetric analysis. A predetermined mass of the sample was weighed, dried in a laboratory oven at 150 °C for 1 h to remove water and volatile components, and then reweighed. The mass of the remaining dried residue was used to calculate the total solid content.The solid content percentage was calculated according to equation 1:

$$\text{Solid content (\%)} = \frac{\text{sample weight after drying}}{\text{sample weight before drying}} \text{ x } 100\ \% \quad (1)$$

2.7. Coating weight

Coating weight was measured to evaluate the uniformity and homogeneity of the coating layer applied to each substrate. Coatings were applied using a #0 bar coater onto paper substrates measuring 10 × 13 cm. Each substrate was weighed before coating and reweighed after complete drying.The percentage increase in substrate weight after coating was calculated using equation 2. The percentage increase in the weight of the substrate after coating was determined using equation 2,

$$\text{Coating weight} = \frac{(B-A)}{A} \text{ x } 100\% \quad (2)$$

Description:
A: Weight of substrates before coating
B: Weight of substrates after coating

Table 2: Scoring criteria for the blocking resistance test.

Score	Description
1 (Very poor)	Separation is very difficult, severe surface damage occurs
2 (Poor)	Separation is difficult and possible only with applied force, with visible surface damage
3 (Fair)	Separation is relatively easy with moderate or minor surface damage
4 (Good)	Separation is easy with minimal or no surface damage
5 (Excellent)	Separation is easy; no evidence of surface damage is visible; substrate is intact

2.8. Fourier Transform Infrared Spectroscopy (FTIR)

FTIR analysis was performed using a Jasco FTIR-4600 spectrometer to identify functional groups and chemical interactions within the coating matrix. Spectra were collected over the relevant wavenumber range to characterize the chemical structure of the coated substrates.

2.9. Optical microscope

The surface morphology of all paper substrates, including ivory board, kraft paper, and MG paper, was examined using a Keyence VHX-6000 digital optical microscope at a magnification of 300 ×. Observations were performed for all formulations after storage periods of 0, 14, and 28 days to evaluate time-dependent surface changes.

2.10. Optical density

The optical density of black-printed substrates was measured before and after coating application using an X-Rite eXact spectrodensitometer. Measurements were taken atthree locations(top, middle, and bottom) on each substrate to evaluate coating uniformity.

2.11. Sealing strength

Heat-sealing strength was measured using a TP-701-C Heat Seal Tester (Sangyo) at 120, 140, 160, and 180 °C. The sealed specimens were subsequently tested using a Shimadzu Autograph AGS-X (500 N) universal testing machine to determine the force required to separate the sealed layers.

2.12. Coefficient of Friction (CoF)

Dynamic coefficient of friction (μd)was measured using a Param MXD-02 CoF tester. These measurements were conducted to evaluate surface slip behavior and frictional characteristics of the coated substrates.

2.13. Rub resistance

Rub resistance was evaluated using a Param RT-01 rub tester operated at 85 rpm for 50, 100, and 150 cycles. Each test was performed in triplicate. The reduction in color density of the printed substrate was measured to quantify the coating layer's abrasion resistance.

3. Results and Discussion

The results and discussion begin with an evaluation of blocking resistance, followed by an assessment of key quality parameters of the water-based coatings. Anti-blocking agent functions by forming a low-surface-energy layer that reduces interlayer adhesion, thereby facilitating layer separation under pressure and at elevated temperatures. Performance and storage stability were evaluated on ivory board, kraft paper, and MG paper substrates after storage periods of 0, 14, and 28 days.

3.1. Blocking storage

The efficacy of the anti-blocking agent in improving the performance of water-based coatings was evaluated through blocking tests conducted on both kraft and MG papers.

Table 2 presents the scoring criteria for the blocking resistance test, rated on a scale from 1 to 5, where 1 indicates very poor resistance and 5 indicates excellent resistance. The STD formulation exhibited limited blocking resistance, particularly on MG paper (score 2), indicating difficult separation with minor surface damage. Kraft paper showed slightly better performance (score 3), which can be attributed to its higher surface roughness and porosity that reduce the effective contact area between coated layers, consistent with previous reports [8]. The incorporation of PDMS improved performance. The T-1 formulation increased the MG score to 3, indicating easier separation with minimal damage.

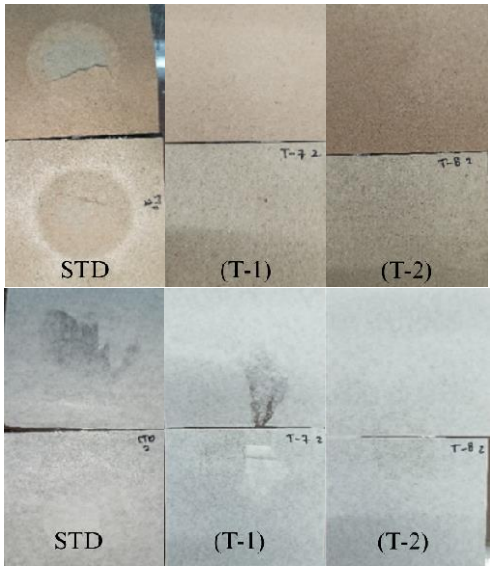

Figure 1: Visual appearance of coated paper samples after the blocking resistancetest.

In contrast, kraft paper achieved a score of 4 ("good"), reflecting only minor surface impairment. Incorporation of PDMS significantly improved anti-blocking performance. Among the tested formulations, T-2, comprising 0.5 g of PDMS, exhibited the highest performance. Both MG paper and kraft paper attained the maximum score of 5 ("excellent"), characterized by effortless separation with no damage to the coating or substrate surfaces. These results indicate that T-2 delivers optimal anti-blocking functionality across various substrates and underscore the critical role of additive concentration in achieving maximum separation and surface protection. The T-1 formulation showed moderate enhancement on both substrates, while the T-2 formulation achieved excellent blocking resistance, with effortless layer separation and no observable surface damage.

The improved performance can be attributed to the intrinsically low surface energy and high chain mobility of PDMS, which reduces interlayer adhesion by promoting the formation of a silicone-rich surface layer during drying [22]. This layer acts as an effective anti-adhesive barrier, suppressing strong interfacial bonding while simultaneously enhancing hydrophobicity and surface durability [23]. Similar effects of organosilicon-based additives in reducing friction and improving handling performance have also been reported in previous studies [24].

Overall, these findings demonstrate that PDMS-based anti-blocking agent, particularly at higher concentrations, offers an effective strategy for improving the handling, storage, and durability of coated paper used in packaging applications.

3.2. Viscosity

The viscosity of the coating formulations during storage is presented in Table 3. Distinct formulation-dependent rheological behaviors were observed over the storage period.

The standard formulation (STD) exhibited a gradual increase in viscosity from day 0 to day 28, which can be attributed to solvent evaporation and progressive interparticle interactions that increase solids concentration and promote network formation. Such behavior is commonly observed in water-based polymer coatings during storage and requires process control to avoid excessive viscosity, which may affect coating efficiency and drying performance [13, 25].

In contrast, formulation T-1 showed pronounced viscosity fluctuations, with a significant increase at day 14 followed by a sharp decrease at day 28. Two-way ANOVA indicated that formulation significantly affected viscosity ($p < 0.001$) and interacted significantly with storage time, whereas storage time alone was not significant ($p = 0.065$). DMRT analysis identified T-1 at day 14 as having the highest viscosity and T-1 at day 28 as the lowest, confirming that T-1 is the least rheologically stable formulation. This behavior indicates dispersion instability, likely due to particle sedimentation or partial phase separation, suggesting that lower PDMS concentration provides limited stabilization and hinders maintenance of a homogeneous particle suspension [26].

Among all formulations, T-2 exhibited the most stable viscosity throughout the storage period, with overlapping statistical groupings across all storage times. This behavior indicates a homogeneous and well-dispersed system, highlighting the effectiveness of higher PDMS content in stabilizing the coating formulation. Similar stabilization effects of organosilicon additives have been reported in previous studies, where increased PDMS concentration reduced storage-induced viscosity variations and improved dispersion stability in water-based coatings [27]. Overall, the results demonstrate that PDMS concentration plays a critical role in governing the rheological stability of water-based coatings during storage, with higher PDMS content providing a more stable viscosity profile suitable for consistent coating application.

Table 3: Viscosity of water-based coatings incorporating anti-blocking agent during storage.

Samples	Viscosity (second)
STD.H-0	25.143 ± 0.20^{a}
STD.H-14	27.637 ± 0.03^{d}
STD.H-28	30.617 ± 0.39^{e}
T-1.H-0	25.860 ± 0.47^{b}
T-1.H-14	31.550 ± 0.25^{f}
T-1.H-28	24.697 ± 0.74^{a}
T-2.H-0	28.083 ± 0.37^{d}
T-2.H-14	26.840 ± 0.14^{c}
T-2.H-28	27.460 ± 0.31^{cd}

*Different letters indicate statistically significant differences between means ($p < 0.05$) as determined by Duncan's multiple range test (DMRT).

3.3. Solid content

The results for solid content are presented in Table 4. The standard formulation (STD) exhibited the lowest and most stable solid content throughout storage. This behavior can be attributed to the absence of anti-blocking agent, which limits changes in dispersion structure and reduce susceptibility to solvent-driven phase separation during storage [28]. Conversely, formulation T-1 demonstrated a significant increase in solid content by day 28, suggesting instability likely linked to insufficient anti-blocking concentrations, which accelerated solvent evaporation and facilitated phase separation [29]. Among all formulations, T-2 showed the most stable solid content throughout the storage period. This stability suggests that a higher concentration of anti-blocking agent helps maintain a balanced solid–liquid phase distribution within the coating system. Stable solid content is essential for achieving consistent coating thickness, predictable drying behavior, and reliable application performance, particularly under industrial storage conditions [28].

The enhanced stability observed in PDMS-containing formulations can be attributed to PDMS's role in reinforcing the coating matrix and mitigating solvent-induced defects. PDMS and associated additives can reduce phase separation, slow degradation processes, and stabilize dispersion structure during storage [30]. Previous studies have similarly reported that coatings formulated with higher-viscosity or higher-content PDMS exhibit improved resistance to material loss and enhanced stability in aqueous environments, supporting the present findings [31].

Table 4: Solid content of water-based coatings with anti-blocking agentmeasured after storagefor 0, 14, and 28 days.

Samples	Solid content (%)
STD.H-0	31.205 ± 0.40^{a}
STD.H-14	31.311 ± 0.16^{a}
STD.H-28	31.893 ± 0.16^{ab}
T-1.H-0	31.520 ± 0.29^{a}
T-1.H-14	32.080 ± 0.15^{abc}
T-1.H-28	33.456 ± 0.13^{d}
T-2.H-0	32.134 ± 0.37^{abc}
T-2.H-14	32.549 ± 0.24^{bcd}
T-2.H-28	32.976 ± 0.36^{d}

*Different letters indicate statistically significant differences between means ($p < 0.05$) according to Duncan's multiple range test (DMRT).

Statistical analysis using a two-way ANOVA indicated that both formulation type and storage time had a significant effect on solid content ($p < 0.05$), whereas their interaction was not significant ($p = 0.274$). These results suggest that changes in solid content during storage are primarily governed by formulation composition and storage duration rather than their combined interaction.

3.4. Coating weight

The evaluation of coating weight across three formulations, STD (standard), T-1 (incorporating 0.2 g of anti-blocking agent), and T-2 (incorporating 0.5 g of anti-blocking agent), was conducted on three distinct paper types: ivory board, kraft paper, and MG paper. This assessment spanned storage durations of 0, 14, and 28 days, with results presented in Table 5.

Among the substrates, kraft paper consistently exhibited the highest coating weight, which can be attributed to its high surface roughness and porosity that promote capillary-driven absorption of the coating into the fiber network. In contrast, ivory board had the lowest coating weight due to its smooth, dense surface structure, which limits coating retention. The MG paper displayed intermediate behavior, reflecting its moderate roughness and more uniform surface morphology [11, 32]. These findings confirm that substrate morphology is the dominant factor governing coating uptake. Formulation effects were secondary to substrate characteristics. The STD formulation produced the lowest coating weight across all substrates, consistent with its lower viscosity and absence of viscosity-modifying additives. The T-1 formulation showed increased coating weight, particularly after intermediate storage periods, which can be associated with higher viscosity and solid content that promote thicker coating deposition [25]. In contrast, the T-2 formulation resulted in intermediate, yet more stable, coating weights across storage times, indicating that higher PDMS content stabilizes the coating layer without causing excessive penetration into porous substrates.

Although higher coating weight was observed on porous substrates and for certain formulations, increased mass does not necessarily translate to improved coating performance. Excessive penetration into the substrate can reduce surface film uniformity and potentially

compromise barrier properties. Therefore, optimal coating performance depends on achieving a balance between sufficient coating mass and the formation of a coherent and uniform surface film.

Table 5: Coating weight of water-based coatings on ivory board, kraft paper, and MG paper containing 0.2 and 0.5 g of anti-blocking agent measured after storage for 0, 14, and 28 days.

Samples	Coating weight (g/m²)
STD.H-0.IB	3.610 ± 0.55^{a}
STD.H-14.IB	4.327 ± 0.60^{ab}
STD.H-28.IB	4.453 ± 0.43^{ab}
T-1.H-0.IB	5.040 ± 0.38^{ab}
T-1.H-14.IB	4.343 ± 0.46^{ab}
T-1.H-28.IB	4.767 ± 0.43^{b}
T-2.H-0.IB	4.730 ± 0.65^{ab}
T-2.H-14.IB	5.520 ± 0.04^{b}
T-2.H-28.IB	4.967 ± 0.56^{ab}
STD.H-0.KP	10.897 ± 0.85^{ef}
STD.H-14.KP	10.953 ± 0.24^{ef}
STD.H-28.KP	12.423 ± 0.86^{fg}
T-1.H-0.KP	10.270 ± 0.14^{d}
T-1.H-14.KP	14.270 ± 0.43^{h}
T-1.H-28.KP	12.607 ± 0.52^{fgh}
T-2.H-0.KP	12.597 ± 0.10^{fgh}
T-2.H-14.KP	12.877 ± 0.64^{fgh}
T-2.H-28.KP	13.953 ± 0.11^{gh}
STD.H-0.MP	7.763 ± 0.17c
STD.H-14.MP	8.337 ± 0.37^{c}
STD.H-28.MP	8.020 ± 0.12^{c}
T-1.H-0.MP	7.800 ± 0.20^{c}
T-1.H-14.MP	8.213 ± 0.05^{c}
T-1.H-28.MP	8.170 ± 0.20^{c}
T-2.H-0.MP	7.900 ± 0.16^{c}
T-2.H-14.MP	8.603 ± 0.08^{cd}
T-2.H-28.MP	8.580 ± 0.11^{cd}

*Different letters indicate statistically significant differences between means ($p < 0.05$) according to Duncan's multiple range test (DMRT).

The observed behavior can be explained by the surface-active nature of PDMS and related anti-blocking agent, which primarily acts at the coating–air interface by reducing surface energy and improving spreading and leveling, rather than significantly increasing bulk coating uptake [33]. Consequently, formulation modifications exert a greater influence on coating uniformity and surface functionality than on total coating weight. Statistical analysis using three-way ANOVA revealed that substrate type had the most significant effect on coating weight ($p < 0.001$), followed by formulation ($p = 0.002$) and storage duration ($p = 0.006$). A significant three-way interaction was observed ($p = 0.048$), indicating that the combined effects of substrate, formulation, and storage time modestly influenced coating uptake.Overall, these results demonstrate that coating weight is predominantly determined by substrate morphology, whereas formulation composition and storage stability primarily affect coating uniformity and reproducibility. In this context, the T-2 formulation offers a more balanced performance, maintaining stable coating weight and uniform film formation across different substrates and storage durations, making it more suitable for practical paper-based packaging applications.

3.5. FTIR

The FTIR spectra of all coated paper substrates (ivory board, kraft paper, and MG paper) prepared with different formulations (STD, T-1, and T-2) and stored for various durations are provided in Supporting Data. The spectra provide insights into the chemical interactions between the coating formulations, anti-blocking agent, and paper substrates.All samples exhibited a broad absorption band in the range of 3600-3200 cm^{-1}, corresponding to –OH stretching vibrations associated with cellulose and hydrogen bonding. The intensity of this band increased from the STD formulation to T-1 and T-2, indicating enhanced interaction between the coating matrix and cellulose fibers upon incorporation of PDMS-based anti-blocking agent [22]. This behavior suggests improved interfacial bonding and coating continuity on paper substrates.

Characteristic aliphatic C–H stretching bands were observed in the region of 2950-2850 cm^{-1}, along with Si–CH_3-related vibrations near 1257 cm^{-1}, confirming the presence of PDMS within the coating matrix. These peaks were more pronounced for T-1 and T-2,

reflecting increased incorporation of organosilicon components. In addition, carbonyl (C=O) bands in the 1730-1650 cm^{-1} range were detected in all coated samples, with higher intensities observed for T-2, indicating a more stable retention of ester or acrylic functional groups within the coating system. The region between 1250 and 1000 cm^{-1}, associated with C–O–C and Si–O stretching vibrations, exhibited increased peak intensity and complexity for PDMS-containing formulations, particularly T-2, across all substrates and storage times [34]. This observation suggests the formation of a more interconnected and chemically stable coating network resulting from the effective incorporation of organosilicon-based additives. Substrate- dependent differences were evident in the –OH stretching region, with kraft paper showing higher peak intensities than ivory board and MG paper. This behavior can be attributed to the higher porosity and surface roughness of kraft paper, which promote deeper coating penetration and stronger interfacial interactions with cellulose fibers [35].

Storage time also influenced coating chemistry. Samples stored for 14 days exhibited the highest peak intensities in the aliphatic C–H and carbonyl regions, indicating optimal consolidation of the coating matrix due to solvent evaporation and enhanced inter-molecular interactions. After prolonged storage (28 days), minor peak shifts and increased spectral complexity, particularly in the Si–O and C–O regions, suggest molecular rearrangement and early aging phenomena commonly reported in silicone-modified polymer systems.

These findings demonstrate that increasing PDMS content enhances both polar and nonpolar functional groups within the coating system, strengthening chemical interactions with cellulose substrates and promoting the formation of a chemically stable coating network. The combined effects of formulation composition, substrate morphology, and storage duration are clearly reflected in the FTIR spectra and support the improved functional performance observed in PDMS-containing coatings.

3.6. Optical microscope

The surface morphology of the coated paper substrates, ivory board, kraft paper, and MG paper,was examined using optical microscopy for different formulations (STD, T-1, and T-2) after storage periods of 0, 14, and 28 days (Figures 2-4).

For the ivory board, morphological changes were relatively limited during storage. The coated surfaces remained largely smooth, with only slight increases in surface roughness observed for PDMS-containing formulations at extended storage times. This behavior reflects the dense and low-porosity structure of ivory board, which restricts coating penetration and minimizes time-dependent surface rearrangements.In contrast, kraft paper exhibited more pronounced morphological evolution. Coated surfaces showed clearer fiber outlines and increased surface roughness with storage time, particularly for PDMS-containing formulations. The highly porous, irregular fiber network of kraft paper facilitates deeper coating penetration and stronger mechanical interlocking, resulting in more pronounced surface texture development during storage [36]. MG paper displayed intermediate behavior between ivory board and kraft paper. While the coatings initially appeared uniform, increased surface roughness and localized micro-features became apparent at longer storage times, especially for T-1 and T-2. This behavior suggests that limited penetration, combined with surface-localized coating components, can influence surface stability during storage.

These observations indicate that substrate morphology plays a dominant role in governing coating surface evolution during storage. Highly porous substrates promote stronger coating–fiber interactions, while smoother substrates favor more uniform and stable surface layers. The incorporation of anti-blocking agent influences surface texture development over time, underscoring the need to optimize formulation com-position to balance surface uniformity, durability, and functional performance across different paper substrates [37, 46].

For the MG paper, which has an intermediate surface smoothness, morphological evolution was more pronounced than on ivory board but less controlled than on kraft paper. While day 0 surfaces appeared uniformly coated, samples stored for day 14 and day 28, particularly T-1 and T-2, exhibited increasing roughness, visible fiber outlines, and microcracks. This suggests that limited penetration combined with surface-localized additive accumulation can promote stress development and crack formation during storage.

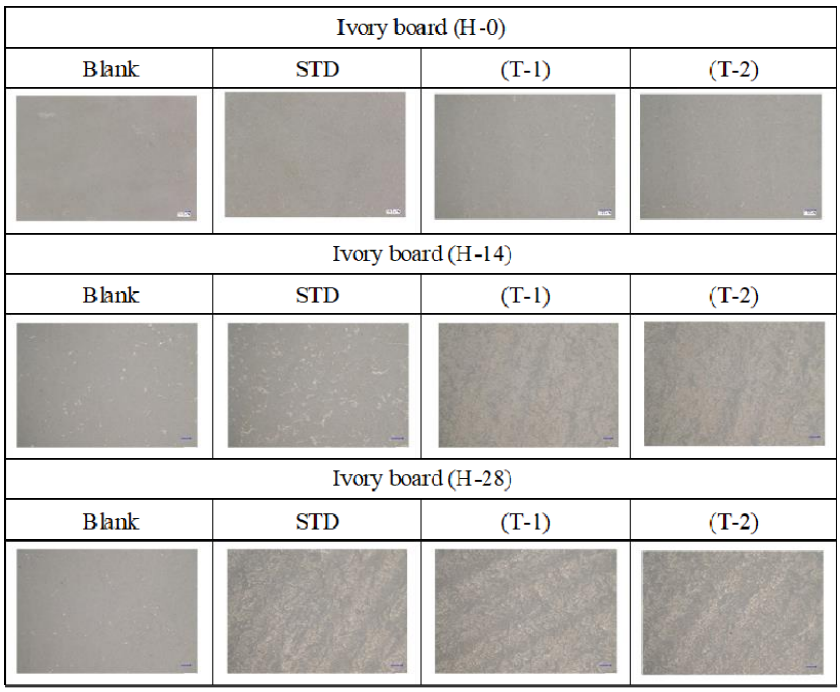

Figure 2: Optical microscopy images showing the effect of formulation and storage time on the surface morphology of ivory board; Scale bar = 100 μm.

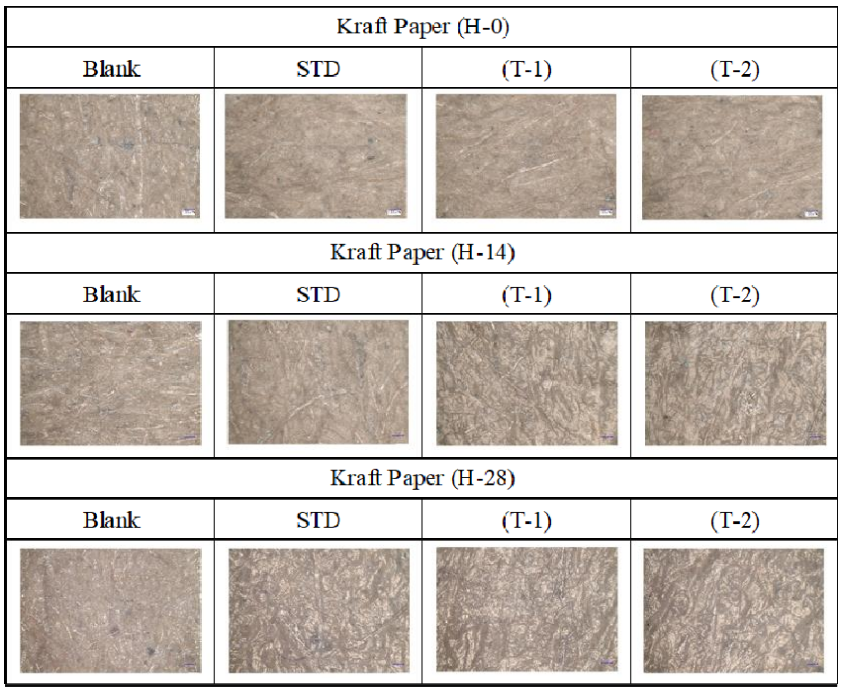

Figure 3: Optical microscopy images showing the effect of formulation and storage time on the surface morphology of kraft paper. Scale bar = 100 μm.

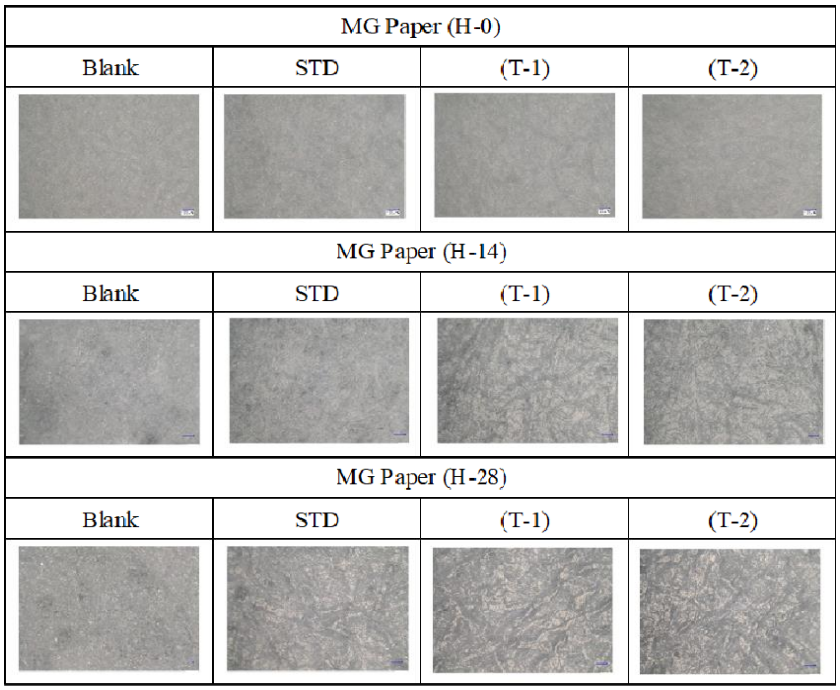

Figure 4: Optical microscopy images showing the effect of formulation and storage time on the surface morphology of MG paper; Scale bar = 100 μm.

The microscopy results demonstrate that substrate morphology critically governs coating stability during storage. High-porosity substrates, such as kraft paper, facilitate additive entrapment and mechanical interlocking, thereby enhancing coating cohesion, durability, and anti-blocking performance [46]. However, formulations containing higher levels of anti-blocking agent (T-1 and T-2) also exhibit increased surface roughness and microcracking over time, indicating a trade-off between improved blocking resistance and long-term surface uniformity. These findings highlight the importance of formulation optimization to balance coating smoothness, mechanical integrity, and durability across substrates with different porosity and surface characteristics [37].

These observations are consistent with previous reports indicating that substrate porosity and surface morphology significantly influence the penetration and final distribution of coating materials in paper-based systems, affecting surface cohesion and texture formation during storage [38]. Migration and segregation phenomena of silicone-based additives to the coating surface have also been documented, demonstrating how such components can localize and modify surface topography during film formation [39]. Furthermore, multiscale morphological features can develop as coatings consolidate and dry on porous substrates, contributing to variations in surface roughness and functional performance [40].

3.7. Optical density

The optical density (OD) values of the coated paper substrates for all formulations are summarized in Table 6. Clear differences in OD were observed among the paper substrates. Ivory Board exhibited high and uniform OD values across all formulations, which can be attributed to its smooth and dense surface that promotes ink holdout and surface retention after coating application [41]. In contrast, kraft paper consistently showed lower optical density values due to its high porosity and rough fiber network, which facilitate ink absorption into the substrate rather than retention at the surface. MG paper displayed intermediate optical density behavior, reflecting its moderate porosity and surface roughness. These trends are consistent with previous studies reporting that substrate porosity significantly influences ink absorption and print density in coated paper systems [42]. Although formulation effects were less pronounced than substrate effects, variations among formulations were substrate-dependent. Formulations with more stable film formation tended to promote improved surface uniformity on denser substrates, whereas on porous substrates the measured optical

density remained influenced by ink penetration effects [43].

The observed variations in optical density are consistent with previous studies reporting that substrate porosity and surface morphology significantly influence ink absorption and print density in coated paper systems [44]. Higher substrate porosity facilitates ink absorption into the fiber network, resulting in lower measured optical density, whereas dense substrates promote ink retention at the surface, leading to higher and more uniform optical density values [45]. Statistical analysis using two-way ANOVA confirmed that substrate type had a highly significant effect on optical density ($p < 0.001$), while the effect of formulation alone was not significant ($p = 0.086$). However, a significant interaction between substrate type and formulation was observed ($p = 0.035$), indicating that the effect of formulation on optical density depends on the substrate type.

3.8. Water resistance

Water resistance was evaluated for the STD, T-1, and T-2 formulations on ivory board (IB), kraft paper (KP), and MG paper (MP) after storage periods of 0, 14, and 28 days. As summarized in Table 7, all samples consistently achieved the maximum water resistance score of 5, regardless of formulation, substrate type, or storage duration.

Table 6: Optical density of water-based coatings on ivory board (IB), kraft paper (KP), and MG paper (MP) with 0.2 and 0.5 g of anti-blocking agent.

Samples	Optical density
STD.IB	1.493 ± 0.00^{c}
STD.KP	1.470 ± 0.00^{b}
STD.MP	1.497 ± 0.02^{c}
T-1.IB	1.500 ± 0.00^{c}
T-1.KP	1.443 ± 0.00^{a}
T-1.MP	1.483 ± 0.01^{bc}
T-2.IB	1.493 ± 0.00^{c}
T-2.KP	1.470 ± 0.01^{b}
T-2.MP	1.483 ± 0.00^{bc}

*Different letters indicate statistically significant differences between means ($p < 0.05$) according to Duncan's multiple range test (DMRT).

Table 7: Water resistance testing of water-based coatings on ivory board (IB), kraft paper (KP), and MG paper (MP) with 0.2 and 0.5 g of anti-blocking agent.

Samples	Water resistance
STD.H-0.IB	$4 \pm 0{,}00^{cd}$
STD.H-14.IB	$4 \pm 0{,}00^{cd}$
STD.H-28.IB	$4 \pm 0{,}00^{cd}$
T-1.H-0.IB	$4 \pm 0{,}00^{cd}$
T-1.H-14.IB	$5 \pm 0{,}00^{e}$
T-1.H-28.IB	$4 \pm 0{,}00^{cd}$
T-2.H-0.IB	$5 \pm 0{,}00^{e}$
T-2.H-14.IB	$5 \pm 0{,}00^{e}$
T-2.H-28.IB	$5 \pm 0{,}00^{e}$
STD.H-0.KP	$3{,}667 \pm 0{,}57^{bcd}$
STD.H-14.KP	$3{,}667 \pm 0{,}57^{bcd}$
STD.H-28.KP	$3{,}333 \pm 0{,}57^{bc}$
T-1.H-0.KP	$3{,}333 \pm 0{,}57^{bc}$
T-1.H-14.KP	$3{,}667 \pm 0{,}57^{bcd}$
T-1.H-28.KP	$4 \pm 0{,}00^{cd}$
T-2.H-0.KP	$2{,}667 \pm 0{,}57^{a}$
T-2.H-14.KP	$3{,}667 \pm 0{,}57^{bcd}$
T-2.H-28.KP	$3{,}333 \pm 0{,}57^{bc}$
STD.H-0.MP	$4 \pm 0{,}00^{cd}$
STD.H-14.MP	$4 \pm 0{,}00^{cd}$
STD.H-28.MP	$4{,}333 \pm 0{,}57^{d}$
T-1.H-0.MP	$4 \pm 0{,}00^{cd}$
T-1.H-14.MP	$3{,}667 \pm 0{,}57^{bcd}$
T-1.H-28.MP	$4 \pm 0{,}00^{cd}$
T-2.H-0.MP	$3 \pm 0{,}00^{ab}$
T-2.H-14.MP	$4 \pm 0{,}00^{cd}$
T-2.H-28.MP	$4 \pm 0{,}00^{cd}$

Due to the absence of variation among the measured values, ANOVA was not applicable because identical values resulted in zero variance and rendered the F-test invalid. The uniform results indicate that all coating formulations provide excellent resistance to water penetration under the tested conditions. The consistently high water resistance confirms that the base water-based coating possesses strong inherent barrier properties. Importantly, the incorporation of PDMS-based anti-blocking agent at both low (T-1) and higher

(T-2) concentrations did not compromise water resistance, even after extended storage. PDMS is known to reduce surface energy and promote the formation of continuous hydrophobic surface layers, effectively limiting water ingress on paper substrates [11]. Similar behavior has been reported in previous studies, where PDMS- or silicone-modified water-based coatings maintained stable water resistance despite variations in formulation and storage conditions [46]. These results are consistent with the viscosity and microscopy findings, suggesting that variations in substrate morphology and storage did not adversely affect water barrier performance under the tested conditions.The results demonstrate that PDMS-based anti-blocking agent can be incorporated into water-based coatings without sacrificing moisture resistance, while simultaneously providing additional anti-blocking functionality suitable for durable and eco-friendly paper packaging applications.

3.9. Oil resistance

The oil resistance of all coating formulations (STD, T-1, and T-2) on all substrates is presented in Table 8. The results indicate that substrate type is the dominant factor governing oil resistance, while the effects of formulation and storage time are strongly substrate-dependent.Ivory board consistently exhibited the highest oil resistance, particularly for PDMS-containing formulations, reflecting its smooth surface and low porosity, which favor the formation of a continuous surface barrier against oil penetration. In contrast, kraft paper showed the lowest oil resistance values across most formulations and storage conditions. This behavior is attributed to its high porosity and rough fiber network, which promotes coating penetration into the substrate rather than surface film formation. MG paper exhibited intermediate oil resistance, consistent with its moderate porosity and surface characteristics. Statistical analysis using three-way ANOVA confirmed that substrate type had a highly significant effect on oil resistance ($p < 0.001$), followed by storage time ($p = 0.003$). At the same time, formulation alone was not statistically significant ($p = 0.672$). Significant interaction effects between formulation and substrate, as well as among formulation, substrate, and storage time, indicate that the performance of PDMS-containing coatings depends strongly on substrate characteristics and storage conditions. Storage generally improved oil resistance, particularly after 14 and 28 days, likely due to coating consolidation and reduced pore accessibility; however, for highly porous kraft paper, oil resistance remained limited even after extended storage. Further analysis indicates that differences between T-1 and T-2 are substrate-dependent. On the ivory board, T-2 consistently exhibited higher and more stable oil resistance than

Table 8: Oil resistance of coatings containing 0.2 and 0.5 g of anti-blocking agent on ivory board (IB), kraft paper (KP), and MG paper (MP) measured after storage for 0, 14, and 28 days.

Samples	Oil Resistance
STD.H-0.IB	$4 \pm 0{,}00^{cd}$
STD.H-14.IB	$4 \pm 0{,}00^{cd}$
STD.H-28.IB	$4 \pm 0{,}00^{cd}$
T-1.H-0.IB	$4 \pm 0{,}00^{cd}$
T-1.H-14.IB	$5 \pm 0{,}00^{e}$
T-1.H-28.IB	$4 \pm 0{,}00^{cd}$
T-2.H-0.IB	$5 \pm 0{,}00^{e}$
T-2.H-14.IB	$5 \pm 0{,}00^{e}$
T-2.H-28.IB	$5 \pm 0{,}00^{e}$
STD.H-0.KP	$3{,}667 \pm 0{,}57^{bcd}$
STD.H-14.KP	$3{,}667 \pm 0{,}57^{bcd}$
STD.H-28.KP	$3{,}333 \pm 0{,}57^{bc}$
T-1.H-0.KP	$3{,}333 \pm 0{,}57^{bc}$
T-1.H-14.KP	$3{,}667 \pm 0{,}57^{bcd}$
T-1.H-28.KP	$4 \pm 0{,}00^{cd}$
T-2.H-0.KP	$2{,}667 \pm 0{,}57^{a}$
T-2.H-14.KP	$3{,}667 \pm 0{,}57^{bcd}$
T-2.H-28.KP	$3{,}333 \pm 0{,}57^{bc}$
STD.H-0.MP	$4 \pm 0{,}00^{cd}$
STD.H-14.MP	$4 \pm 0{,}00^{cd}$
STD.H-28.MP	$4{,}333 \pm 0{,}57^{d}$
T-1.H-0.MP	$4 \pm 0{,}00^{cd}$
T-1.H-14.MP	$3{,}667 \pm 0{,}57^{bcd}$
T-1.H-28.MP	$4 \pm 0{,}00^{cd}$
T-2.H-0.MP	$3 \pm 0{,}00^{ab}$
T-2.H-14.MP	$4 \pm 0{,}00^{cd}$
T-2.H-28.MP	$4 \pm 0{,}00^{cd}$

*Different letters indicate statistically significant differences between means ($p < 0.05$) according to Duncan's multiple range test (DMRT).

T-1 across storage periods, indicating that a higher PDMS content promotes the formation of a more continuous and effective surface barrier on smooth, low-porosity substrates. In contrast, on kraft paper, increasing PDMS content did not lead to proportional improvements in oil resistance, suggesting that excessive penetration into the porous fiber network limits surface film continuity.

Storage time also influenced oil resistance behavior. The improvements observed at 14 and 28 days, particularly for PDMS-containing formulations on ivory board, likely reflect coating consolidation and reduced pore accessibility during storage. However, for highly porous substrates such as kraft paper, oil resistance remained limited even after extended storage, indicating that storage-induced densification cannot fully compensate for substrate-driven penetration effects. The enhancement of oil resistance by PDMS is primarily associated with its ability to lower surface energy and form hydrophobic, low-adhesion surface layers, which is most effective on smooth substrates where PDMS can readily concentrate at the coating–air interface [16]. On highly porous substrates such as kraft paper, partial infiltration of PDMS into the fiber network reduces surface layer continuity, thereby limiting oil barrier effectiveness [47]. Similar findings have been reported for PDMS-modified and water-based barrier coatings, in which substrate porosity was identified as the primary limiting factor for oil resistance [36].

3.10. Coefficient of Friction (CoF)

The results of the CoF test for all formulations and substrates are presented in Table 9. The results indicate that substrate type is the dominant factor governing friction behavior, while the effects of formulation and storage time are strongly substrate-dependent.Across the investigated paper substrates, PDMS-containing formulations (T-1 and T-2) consistently exhibited lower CoF values than the standard formulation (STD), confirming the effectiveness of PDMS as a slip and anti-blocking agent. Ivory board showed the lowest CoF values, particularly for T-1 and T-2 after 14 and 28 days of storage. This behavior is attributed to its smooth surface and low porosity, which favor PDMS migration and accumulation at the coating-air interface, thereby reducing surface energy and enhancing slip performance. Kraft paper exhibited higher CoF values than ivory board across most formulations and storage times. The rough and porous fiber network of kraft paper promotes partial penetration of the coating and PDMS into the substrate, limiting the formation of a continuous lubricating surface layer and reducing the effectiveness of friction reduction. MG paper showed intermediate CoF behavior, consistent with its moderate surface roughness and porosity.

Table 9: Dynamic CoF of coatings with 0.2 and 0.5 g of anti-blocking agent on ivory board (IB), kraft paper (KP), and MG paper (MP) measured after storage for 0, 14, and 28 days.

Samples	CoF (μd)
STD.H-0.IB	$0,43 \pm 0,03^{m}$
STD.H-14.IB	$0,353 \pm 0,02^{k}$
STD.H-28.IB	$0,325 \pm 0,01^{ij}$
T-1.H-0.IB	$0,307 \pm 0,01^{hi}$
T-1.H-14.IB	$0,126 \pm 0,00^{a}$
T-1.H-28.IB	$0,15 \pm 0,00^{abcd}$
T-2.H-0.IB	$0,216 \pm 0,01^{fg}$
T-2.H-14.IB	$0,123 \pm 0,00^{a}$
T-2.H-28.IB	$0,139 \pm 0,00^{ab}$
STD.H-0.KP	$0,397 \pm 0,03^{l}$
STD.H-14.KP	$0,421 \pm 0,01^{lm}$
STD.H-28.KP	$0,334 \pm 0,02^{jk}$
T-1.H-0.KP	$0,196 \pm 0,01^{ef}$
T-1.H-14.KP	$0,162 \pm 0,00^{bcd}$
T-1.H-28.KP	$0,176 \pm 0,01^{de}$
T-2.H-0.KP	$0,225 \pm 0,00^{g}$
T-2.H-14.KP	$0,16 \pm 0,00^{bcd}$
T-2.H-28.KP	$0,144 \pm 0,00^{abc}$
STD.H-0.MP	$0,404 \pm 0,02^{lm}$
STD.H-14.MP	$0,295 \pm 0,00^{h}$
STD.H-28.MP	$0,355 \pm 0,01^{k}$
T-1.H-0.MP	$0,176 \pm 0,00^{de}$
T-1.H-14.MP	$0,128 \pm 0,01^{a}$
T-1.H-28.MP	$0,17 \pm 0,00^{de}$
T-2.H-0.MP	$0,206 \pm 0,00^{fg}$
T-2.H-14.MP	$0,127 \pm 0,01^{a}$
T-2.H-28.MP	$0,143 \pm 0,00^{abc}$

Storage time had a pronounced effect on CoF, particularly for PDMS-containing formulations. CoF values generally decreased after 14 days of storage, indicating progressive coating consolidation and enhanced surface enrichment of PDMS, with silicone additives exhibiting time-dependent migration toward the coating surface, thereby reducing friction and improving slip properties [48]. The lowest CoF values were observed at day 14 for both T-1 and T-2 across all substrates, indicating an optimal balance between coating stabilization and additive migration. Slight increases at day 28 may be associated with surface rearrangement or partial additive redistribution during extended storage. Statistical analysis using three-way ANOVA confirmed that substrate type had a highly significant effect on CoF ($p < 0.001$), followed by formulation ($p < 0.001$) and storage time ($p < 0.01$). Significant interaction effects among formulation, substrate, and storage time indicate that friction-reduction efficiency depends on the combined effects of surface morphology, additive concentration, and storage conditions. Duncan's multiple range test further showed that the lowest CoF values were consistently achieved by PDMS-containing formulations on smooth substrates after intermediate storage times.

The reduction in CoF observed for PDMS-containing formulations is consistent with previous studies reporting that silicone-based additives migrate toward the coating surface, forming a low-surface-energy lubricating layer that enhances slip and anti-blocking performance [49]. The effectiveness of this mechanism is strongly substrate-dependent, with smooth, low-porosity surfaces favoring surface enrichment of PDMS, while porous substrates limit friction reduction due to additive penetration into the fiber network [50].

3.11. Sealing strength

The results of sealing strength measurements for all formulations and substrates are presented in Table 10. The results in Table 10 demonstrate that substrate type is the primary determinant of sealing strength, followed by storage time, while formulation effects are strongly substrate-dependent. Kraft paper consistently exhibited the highest sealing strength, with the maximum values observed at extended storage times. Despite its high porosity, kraft paper promotes deep coating penetration, enabling effective pore filling and strong mechanical interlocking during thermal sealing.

Table 10: Sealing strength of coatings with 0.2 and 0.5 g anti-blocking agent on ivory board (IB), kraft paper (KP), and MG paper (MP) measured after storage for 0, 14, and 28 days.

Samples	Sealing strength (N/m)
STD.H-0.IB	415,667 ± 56,04^{de}
STD.H-14.IB	460,667 ± 38,85^{ef}
STD.H-28.IB	573,333 ± 30,08^{hi}
T-1.H-0.IB	510,333 ± 39,52^{fgh}
T-1.H-14.IB	459 ± 26,66^{ef}
T-1.H-28.IB	537,667 ± 38,00^{gh}
T-2.H-0.IB	527,333 ± 37,81^{fgh}
T-2.H-14.IB	548,333 ± 6,65^{ghi}
T-2.H-28.IB	524,667 ± 32,34^{fgh}
STD.H-0.KP	382,333 ± 31,56^{d}
STD.H-14.KP	573,667 ± 38,85^{hi}
STD.H-28.KP	622 ± 74,64^{i}
T-1.H-0.KP	375 ± 24,02^{e}
T-1.H-14.KP	563,333 ± 37,20^{hi}
T-1.H-28.KP	535,667 ± 72,00^{gh}
T-2.H-0.KP	363,667 ± 26,08^{d}
T-2.H-14.KP	474 ± 29,46^{efg}
T-2.H-28.KP	589 ± 60,55^{hi}
STD.H-0.MP	164,667 ± 43,93^{a}
STD.H-14.MP	141 ± 14,93^{a}
STD.H-28.MP	276 ± 11,26^{bc}
T-1.H-0.MP	169,333 ± 36,22^{a}
T-1.H-14.MP	134,333 ± 21,03^{a}
T-1.H-28.MP	242,667 ± 45,78^{bc}
T-2.H-0.MP	153,667 ± 14,57^{a}
T-2.H-14.MP	206,333 ± 59,40^{ab}
T-2.H-28.MP	283 ± 48,50^{c}

*Different letters indicate statistically significant differences between means ($p < 0.05$) according to Duncan's multiple range test (DMRT).

This interlocking mechanism enhances stress distribution and peel resistance, resulting in superior sealing performance when sufficient coating consolidation is achieved. Similar behavior has been reported for porous substrates, where adequate coating infiltration improves adhesion and seal integrity. Ivory board also

exhibited high sealing strength, particularly for PDMS-containing formulations at 14 and 28 days of storage, as well as for the standard formulation after extended storage. The dense, smooth surface of ivory board facilitates uniform coating deposition and efficient heat transfer during sealing, resulting in strong, consistent thermal bonds [51]. In contrast, MG paper consistently showed the lowest sealing strength values. Its thin structure and lower mechanical integrity limit load-bearing capacity during sealing and hinder the formation of robust interfacial bonds, making it more susceptible to cohesive or substrate failure [52].

Among the formulations, T-2 generally provided the most consistent improvement in sealing strength, especially on kraft paper and ivory board. The higher PDMS content is expected to enhance interfacial compliance and coating cohesion, allowing better accommodation of thermal stresses during sealing. However, the formulation alone was not statistically significant ($p=0.370$), indicating that PDMS's contribution to sealing strength is governed by its interaction with substrate morphology and storage-induced film maturation rather than by concentration alone.

Storage time had a significant effect on sealing strength ($p < 0.001$), with higher values generally observed after 14 and 28 days of storage. This improvement is attributed to solvent evaporation, coating consolidation, and further film stabilization, which enhance cohesive strength within the coating layer and adhesion to the substrate [53]. These effects were most pronounced on kraft paper and ivory board, where mechanical interlocking and uniform surface bonding dominate the sealing mechanism.

Three-way ANOVA confirmed significant effects of substrate type ($p < 0.001$) and storage time ($p < 0.001$), as well as significant formulation × substrate, storage × substrate, and three-way interactions ($p < 0.05$). Duncan's multiple-range test indicated that coatings on kraft paper achieved the highest sealing strength after extended storage, while MG paper exhibited the lowest sealing performance across formulations.

These results demonstrate that sealing strength is governed by substrate morphology, coating consolidation, and formulation–substrate interactions. Porous substrates, such as kraft paper, benefit from coating penetration and mechanical interlocking, whereas smooth substrates, such as ivory board, rely on uniform film formation and efficient thermal bonding. The combination of PDMS-containing formulations and adequate storage time provides robust sealing performance, emphasizing the importance of tailoring coating formulation and processing conditions to substrate characteristics for optimized heat-sealing efficiency in paper-based packaging applications.

3.12. Rub resistance

Rub resistance tests were carried out for three coating formulations of STD, T-1 (0.2 g anti-blocking), and T-2 (0.5 g anti-blocking) on ivory board (IB), kraft paper (KP), and MG paper (MP) substrates. The results are summarized in Table 11.

As shown in Table 11, the incorporation of the anti-blocking agent improved overall rub resistance, confirming its effectiveness in enhancing the mechanical durability of the coating layer. Among the substrates, MG paper exhibited the most pronounced response to anti-blocking addition, showing a clear increase in rub resistance from the standard formulation to PDMS-containing formulations. This behavior suggests that MG paper provides favorable surface and fiber characteristics for forming a flexible yet abrasion-resistant coating film. Ivory board also showed a progressive increase in rub resistance from STD to T-2, although the magnitude of improvement was less pronounced than that observed for MG paper. This trend can be attributed to the dense, smooth surface of ivory board, which limits coating adhesion and delays the development of maximum abrasion resistance.

Table 11: Rub resistance testing of water-based coatings with 0.2 and 0.5 g of anti-blocking on ivory board (IB), kraft paper (KP), and MG paper (MP) substrates.

Samples	Rub Resistance
STD.IB	$94{,}539 \pm 0{,}32^{a}$
STD.KP	$97{,}166 \pm 0{,}95^{bc}$
STD.MP	$95{,}904 \pm 0{,}93^{ab}$
T-1.IB	$95{,}531 \pm 1.05^{ab}$
T-1.KP	$96{,}922 \pm 2.10^{bc}$
T-1.MP	$98{,}672 \pm 1.31^{c}$
T-2.IB	$96{,}756 \pm 0{,}62^{abc}$
T-2.KP	$97{,}354 \pm 1.74^{bc}$
T-2.MP	$98{,}444 \pm 1.04^{c}$

* The different letters indicate that the means are significantly ($p < 0.05$) by Duncan's multiple range tests.

In contrast, kraft paper exhibited relatively stable rub resistance across formulations. Its high porosity promotes coating penetration into the fiber network rather than surface film build-up, thereby reducing the rub resistance's sensitivity to formulation changes. At lower anti-blocking content (T-1), penetration effects dominate, whereas at higher loading (T-2), sufficient coating material remains at the surface to improve abrasion resistance. Among the formulations, T-2 provided the most stable and consistently high rub resistance across all substrates, indicating that higher PDMS content promotes the formation of a denser, more cohesive, and flexible surface layer capable of resisting mechanical wear [53]. In contrast, the standard formulation consistently exhibited the lowest rub resistance, highlighting the critical role of anti-blocking agent in reinforcing surface durability.

Statistical analysis using a two-way ANOVA confirmed that both substrate type ($p = 0.006$) and formulation ($p = 0.030$) significantly influenced rub resistance, whereas the interaction was not significant ($p = 0.252$). This indicates that substrate characteristics (such as porosity, roughness, and fiber structure) and anti-blocking content independently govern abrasion resistance.

These findings are consistent with previous studies reporting that PDMS-based additives form smooth, flexible, low-friction surface layers that reduce frictional stress and enhance resistance to mechanical wear [54]. In the present study, the superior performance of the T-2 formulation confirms that higher anti-blocking content strengthens the coating matrix and improves abrasion resistance, while substrate morphology modulates the magnitude of this improvement.

4. Conclusion

This study demonstrates that incorporating an anti-blocking agent, particularly PDMS, effectively enhances the stability, processability, and functional performance of water-based coatings applied to paper substrates for sustainable packaging applications. The results show that coating performance is not determined solely by formulation, but by the combined effects of additive concentration, substrate morphology, and storage duration.Among the formulations investigated, the higher anti-blocking content (T-2) provided the most balanced and reliable performance, characterized by stable viscosity and solid content during storage, reduced surface friction, improved rub resistance, and enhanced sealing strength, while maintaining excellent water and oil resistance. These findings indicate that optimal coating performance is achieved by forming a uniform, coherent, and mechanically stable surface layer rather than by increasing coating weight alone. Substrate-dependent behavior was clearly observed. Smooth, dense substrates favored continuous surface film formation, whereas more porous papers promoted coating penetration and mechanical interlocking, thereby significantly influencing adhesion and sealing efficiency. The present findings indicate that water-based paper coating formulations can be effectively tailored to specific substrate characteristics and processing requirements in converting operations. The multifunctional role of PDMS-based anti-blocking agent demonstrated in this work highlights their strong potential as effective additives in eco-friendly paper packaging systems. Future studies should focus on long-term aging behavior, recyclability, and repulpability, as well as on exploring synergistic combinations with bio-based or nanostructured additives to improve barrier performance further while maintaining sustainability.

5. References

1. Tanpichai S, Witayakran S, Wootthikanokkhan J, Srimarut Y, Woraprayote W, Malila Y. Mechanical and antibacterial properties of chitosan-coated cellulose paper for packaging applications: effects of molecular weight types and concentrations of chitosan. Int J Biol Macromol**.** 2020; 155:1510–1519. https://doi.org/10.1016/j.ijbiomac.2019.11.128.
2. Setajit C, Kongvarhodom C, Xiao H. Development of grease-resistant packaging paper using cellulose nanocrystals and sodium alginate. Sci Adv Mater**.** 2020; 12(2):212–219. https://doi.org/10.1166/sam. 2020.3628.
3. Lignou S, Oloyede OO. Consumer acceptability and sensory profile of sustainable paper-based packaging. Foods**.** 2021;10(5):990. .https://doi.org/10.3390/foods 10050990
4. Kunam PK, Ramakanth D, Akhila K, Gaikwad KK. Bio-based materials for barrier coatings on paper packaging. Biomass Convers Biorefin. 2024;14(12): 12637-12652. https://doi.org/10.1007/s13399-022-03241-2.
5. Zhang W, Xiao H, Qian L. Enhanced water vapour barrier and grease resistance of paper bilayer-coated with chitosan and beeswax. Carbohydr Polym**.** 2014; 101(1):401-406. https://doi.org/10.1016/j.carbpol. 2013.

09.097.
6. Lo Faro E, Menozzi C, Licciardello F, Fava P. Improvement of paper resistance against moisture and oil by coating with poly(3-hydroxybutyrate-co-3-hydroxyvalerate) and polycaprolactone. Appl Sci**.** 2021; 11(17):8058. https://doi.org/10.3390/app111780 58.
7. Lo Faro E, Bonofiglio A, Barbi S, Montorsi M, Fava P. Polycaprolactone/starch/agar coatings for food-packaging paper: statistical correlation of the formulations' effect on diffusion, grease resistance, and mechanical properties. Polymers**.** 2023; 15(19):3921. https://doi.org/10.3390/polym15193921.
8. Marinelli A, Profaizer M, Diamanti MV, Pedeferri MP, Del Curto B. Heat-seal ability and fold cracking resistance of kaolin-filled styrene–butadiene-based aqueous dispersions for paper-based packaging. Coat. 2023; 13(6):975. https://doi.org/10.3390/coatings13060 975.
9. Luo H, Zhang S, Li X, Wang J, Chen L. Anti-smudge and self-cleaning characteristics of waterborne polyurethane coatings modified with silicone additives. J Colloid Interface Sci. 2022;628:1070-1081. https://doi. org/10.1016/j.jcis.2022.08.017.
10. Agustina LA, Lestari YD, Adhinanda AA, Ariesta MN. Study of inorganic-based anti-blocking agents as migration control of slip additives on the surface of polyethylene monolayer films. Acta Chim Asiana. 2024;7:366-376. https://doi.org/10.29303/aca.v7i1. 196
11. Kumar V, Koppolu VR, Bousfield D, Toivakka M. Substrate role in coating of microfibrillated cellulose suspensions. Cellulose. 2017;24(3):1247-1260. https:// doi.org/10.1007/s10570-017-1201-5.
12. Sharma M, Aguado R, Murtinho D, Valente A, Ferreira P. Micro-/nanofibrillated cellulose-based coating formulations: a solution for improving paper printing quality. Nanomaterials**.** 2022;12(16):2853. https://doi.org/10. 3390/nano12162853.
13. Aloui H, Khwaldia K. Effects of coating weight and nanoclay content on functional and physical properties of bionanocomposite-coated paper. Cellulose**.** 2017; 24(10):4493-4507. https://doi.org/10.1007/s10570-017-1436-1.
14. Sun G, Qian C, Li Z, Wang Q. Optimizing powder-to-liquid ratios in lost foam casting coatings: impacts on viscosity, shear-thinning behavior, coating weight, and surface morphology. Coatings. 2024;14(9):1089. https://doi.org/10.3390/coatings14091089.
15. Benz B, Burton D, Ventresca D, Welsch G. Optimizing water and water vapor barrier properties of water-based barrier coatings. TAPPI J. 2025;24(1):7–23.
16. Khlewee M, Desisto W, Bousfield DW. Water-based adhesive penetration into paperboard and coated paperboard. TAPPI J. 2025;24(1):48–54.
17. Lin CB, Chang HS, Zhang Y, Yang F, Lee S. Spreading of water droplets on cellulose-based papers: the effect of back-surface coating. Langmuir. 2021;37 (1):e10291. https://doi.org/10.1021/acs.langmuir.0c02 991.
18. Bolvardi B, Seyfi J, Hejazi I, Otadi M, Khonakdar HA, Davachi SM. Towards an efficient and durable superhydrophobic mesh coated by PDMS/TiO_2 nanocomposites for oil/water separation. Appl Surf Sci. 2019; 492:143-152. https://doi.org/10.1016/j.apsusc. 2019.06.268.
19. Huang J, Cai P, Li M, Wu Q, Li Q, Wang S. Preparation of CNF/PDMS superhydrophobic coatings with good abrasion resistance. Materials. 2020;13 (23):5380. https://doi.org/10.3390/ma13235380.
20. Yue D, Lin S, Cao M, Lin W, Zhang X. Fabrication of transparent and durable superhydrophobic poly-siloxane/SiO_2 coating on the wood surface. Cellulose. 2021; 28(6):3745-3758. https://doi.org/10. 1007/s10570-021-03758-1.
21. Lavoine N, Desloges I, Dufresne A, Bras J. Microfibrillated cellulose: its barrier properties and applications in cellulosic materials—A review. Carbohydr Polym. 2012;90(2):735–764. https://doi. org/ 10.1016/j.carbpol.2012.05.026.
22. Kumar D, Wu X, Fu Q, Weng J, Ho C, Kanhere PD, et al. Hydrophobic sol-gel coatings based on poly-dimethylsiloxane for self-cleaning applications. Mater Des. 2015;86:855-862. https://doi.org/10.1016/j. matdes. 2015.07.174.
23. Joki-Korpela F, Pakkanen TT. Incorporation of polydimethylsiloxane into polyurethanes and characterization of copolymers. Eur Polym J. 2011;47(8): 1694-1708. https://doi.org/10.1016/j.eurpolymj. 2011. 06.006.
24. Palumbo F, Lo Porto C, Favia P. Plasma nano-texturing of polymers for wettability control: why, what and how. Coatings. 2019;9(10):640. https://doi. org/ 10.3390/ coatings9100640.
25. Dixit N, Maloney KM, Kalonia DS. Effect of processing parameters on the physical stability of silicone coatings. AAPS Pharm Sci Tech. 2012; 13(4): 1116–1124. https://doi.org/10.1208/s12249-012-9842-7.
26. Sun G, Wang Q, Li S. Influence of mixing and standing times on the rheological properties of shell casting coatings. Coatings. 2024;14(8):954. https://doi.org/10. 3390/coatings14080954.
27. Yan X, Li M, Zhao M, Zhou H, Wang Y. Effect of PDMS viscosity and curing agent content on the mechanical properties of PDMS fouling-release coatings. J Phys Conf Ser. 2022; 2174:012036. https://doi.org/10.1088/1742-6596/2174/1/012036.
28. Xia Y, Zhu N, Zhao Y, et al. Construction of durable self-cleaning PDMS film on polyester fabric surface. Materials. 2023;16(2):52. https://doi.org/10.3390/ma 16020052.
29. Fang J, Dong R, Zhou M, Liang L, Yang M, Xing H, et al. Hydrophobic, durable, and reprocessable PEDOT: PSS/PDMS–PUa/SiO_2 film with conductive self-cleaning and de-icing functionality. Coatings. 2025; 15:90985. https://doi.org/10.3390/coatings150 90985
30. Li Z, Rabnawaz M. Fabrication of food-safe water-resistant paper coatings using a melamine primer and polysiloxane outer layer. ACS Omega. 2018; 3:e00106. https://doi.org/10.1021/acsomega.8b00106

31. Ji X, Wang H, Ma X, He C, Guo M. Progress in poly-dimethylsiloxane-modified waterborne poly-urethanes. RSC Adv. 2017;7:34086-34095. https://doi.org/10. 1039/ C7RA04768A.
32. Jutila E, Koivunen R, Gane PAC. Effect of coating pigment, binder type and binder amount on planar liquid wicking on coated substrates. Nord Pulp Pap Res J. 2015; 30(2):173–186. https://doi.org/10. 14622/JPMTR-1419.
33. Eduok U, Faye O, Szpunar J. Recent developments and applications of protective silicone coatings: a review of PDMS functional materials. Prog Org Coat. 2017;111: 124-163. https://doi.org/10.1016/j.porgcoat.2017.05.012.
34. Tarigan JBR, Nainggolan I, Kaban J. The physico-chemical and antibacterial properties of galactomannan edible films. J Phys Conf Ser. 2018; 1116(1):012035.
35. Croll SG. Surface roughness profile and its effect on coating adhesion and corrosion protection: a review. Prog Org Coat. 2020; 148:105847. https://doi.org/10. 1016/j.porgcoat.2020.105847.
36. Samyn P. Wetting and hydrophobic modification of cellulose surfaces for paper applications. Bio Resources. 2013; 8(3):4323–4344.
37. Ghaffar SH, Madyan OA, Fan M, Corker J. The influence of additives on the interfacial bonding mechanisms between natural fibre and biopolymer composites. Compos B Eng. 2018; 152:1-10. https://doi.org/10.1016/j.compositesb.2018.06.020
38. Aslannejad H, Hassanizadeh SM, Raoof A, de Winter DAM, Tomozeiu N. Characterizing the hydraulic properties of paper coating layer using FIB-SEM tomography and 3D pore-scale modeling. Chem Eng Sci. 2017; 160:275-280. https://doi.org/10.1016/j. ces.2016.11.021
39. Hinder SJ, Lowe C, Maxted JT, Watts JF. Migration and segregation phenomena of a silicone additive in a multilayer organic coating. Prog Org Coat. 2005;54 (2): 104-112.https://doi.org/10.1016/j.porgcoat.2005.06. 001.
40. Samyn P, Van Erps J, Thienpont H, Schoukens G. Paper coatings with multi-scale roughness evaluated at different sampling sizes. Appl Surf Sci. 2011;257: 5613-5625. https://doi.org/10.1016/j.apsusc.2011.01. 059.
41. Thorman S, Ström G, Holmberg K, Järnström PÅ. Uniformity of liquid absorption by coatings: technique and impact of coating composition. Nord Pulp Pap Res J. 2012;27(2):459-465. https://doi.org/10.3183/ npprj-2012-27-02-p459-465.
42. Odhiambo JG, Li W, Zhao Y, Chen C. Porosity and its significance in plasma-sprayed coatings. Coatings. 2019; 9:460. https://doi.org/10.3390/coatings9070460.
43. Keshmiri K, Huang H, Nazemifard N. Compatibility of polydimethylsiloxane microfluidic systems with high-viscosity hydrocarbons. SN Appl Sci. 2019; 1(7):666. https://doi.org/10.1007/s42452-019-0666-2.
44. Rastogi VK, Samyn P. Bio-based coatings for paper applications. Coatings**.** 2015; 5:887-930. https://doi. org/ 10.3390/coatings5040887.
45. Wang X, Tang H, Li X, Hua X. Investigation on mechanical properties of conducting polymer coating–substrate structures. Int J Mol Sci. 2009; 10(12):5257–5284. https://doi.org/10.3390/ijms10125257.
46. Li Z, Rabnawaz M. Oil- and water-resistant coatings for porous cellulosic substrates. ACS Appl Polym Mater. 2018; 6:1234-1243. https://doi.org/10.1021/ acsapm. 8b00106.
47. Neves LB, Afonso S, Nóbrega G, Barbosa LG, Lima RA. Methods to modify PDMS surface wettability and applications: a review. Micromachines. 2024; 15:670. https://doi.org/10.3390/mi15060670.
48. Nugroho A, Kozin M, Mamat R, Bo Z, Fairusham M, Prisla M, et al. Nanoparticle-enriched palm oil biolubricants for enhanced tribological performance. Heliyon. 2024;10(22):e39742. https://doi.org/10.1016/j. heliyon.2024.e39742.
49. Goff J, Sulaiman S, Arkles B. Applications of hybrid polymers generated from living anionic ring-opening polymerization. Molecules. 2021; 26:2755. https://doi. org/10.3390/molecules26092755.
50. Hubbe MA, Szelez S, Venditti RA. Detergency mechanisms and interactions with cellulosic surfaces: a review. BioResources. 2015; 10:7167-7249. https://doi. org/10.15376/biores.17.4.Hubbe.
51. Huang J, Yang M, Wan L, Tang K, Zhang H, Chen J, et al. Ultrafine powder coatings with dense structures and enhanced corrosion resistance. Chem Eng J. 2023; 455:140815. https://doi.org/10.1016/j.cej.2022.140815.
52. Eduok U. Effect of silylating agents on super-hydrophobic and self-cleaning properties of siloxane/ cellulosic fabric filters. RSC Adv. 2021;11: 9586-9599. https://doi.org/10.1039/D0RA10565A.
53. Si C, Cai M, Liu G, Zhang Y, Fan X, Zhu M. PDMS–PI composite coatings for multipurpose tribological applications. Tribol Int. 2023; 189:108919. https://doi. org/10.1016/j.triboint.2023.108919.
54. Lee S, Segu DZ, Kim C. Enhancement of tribological performance of lubricants using polydimethylsiloxane powder additives. RSC Adv. 2024;14:31047-31056. https://doi.org/10.1039/D4RA05164E.

How to cite this article:
Muryeti M, Nur Halisa S. Effect of PDMS Anti-Blocking Agent in Water-Based Coatings on the Performance of Paper Substrates for Sustainable Packaging. Prog Color Colorants Coat. 2026;19(4): 417-434. https://doi.org/10.30509/pccc.2026.167649.1442.